

## Spectroscopic study of an acceptor confined in a narrow GaAs/Al<sub>x</sub>Ga<sub>1-x</sub>As quantum well

P. O. Holtz,\* M. Sundaram, R. Simes, J. L. Merz, A. C. Gossard, and J. H. English

*Department of Electrical and Computer Engineering and Materials Department,  
University of California at Santa Barbara, Santa Barbara, California 93106*

(Received 12 September 1988; revised manuscript received 15 November 1988)

A detailed optical study of the Be acceptor confined at the center of a 70-Å-wide GaAs/Al<sub>0.3</sub>Ga<sub>0.7</sub>As quantum well (QW) is presented in this report. Transitions to the same excited states of this acceptor are observed via two independent spectroscopic techniques: two-hole transitions observed in selective photoluminescence, and resonant Raman scattering. Both of these techniques are well documented from corresponding studies in bulk material, but this is the first report on two-hole transitions observed for acceptor states confined in a QW. Two transitions, interpreted as the transitions from the  $1s_{3/2}(\Gamma_6)$  ground state of the Be acceptor to the excited states,  $2s_{3/2}(\Gamma_6)$  and  $2s_{3/2}(\Gamma_7)$ , respectively, are observed with the two different techniques. The experimentally determined transition energies via the two-hole transitions,  $28.5 \pm 1$  and  $37.0 \pm 1$  meV, respectively, are in good agreement with what is obtained from the resonant Raman-scattering measurements,  $29.0 \pm 0.5$  and  $36.5 \pm 0.5$  meV, respectively. These experimental results are also compared with recent theoretical predictions.

### INTRODUCTION

With the development of the new sophisticated semiconductor growth techniques such as molecular beam epitaxy (MBE) and metalorganic-chemical vapor deposition (MOCVD), the study of superlattices and quantum wells (QW's) has rapidly advanced. These techniques have made it possible to control both the material composition and the impurities on the atomic scale. Original investigations of these structures have been performed with emphasis on undoped QW's, while more recently there has been an increasing interest in the extrinsic properties of doped QW's.<sup>1-8</sup> A photoluminescence (PL) spectrum of a doped QW has similarities but also differences compared with the corresponding PL spectrum of bulk GaAs. In addition to the intrinsic free exciton (FE), features from extrinsic recombination related to impurities such as bound excitons (BE's) and free-to-bound (FB) transitions will appear, but the intensity of the PL of intrinsic origin is strongly enhanced in QW's relative to the extrinsic recombination. Also the electronic configuration for the impurity will be different than in the bulk material, and will vary not only with the well width but also with the position of the impurity in the QW.

The overlap between the electron (hole) confined in the QW and the impurity atom, at which it is bound, will be dependent on the position of the impurity in the QW (or barrier). The variation in binding energy with the impurity position has been calculated in several approximations. The original calculation by Bastard<sup>9</sup> assumed a hydrogenic impurity and infinite barrier height. Recently, more realistic calculations including finite barrier heights have been performed.<sup>10,11</sup> Thus there has been recent progress with respect to the theoretical aspect of this subject, but there have been few experimental demonstra-

tions of the properties of confined impurities. In particular, the information on the position dependence and excited states related to confined impurities is rather limited.

The experimental investigation of impurity levels in QW's should, in principle, not be more difficult than in bulk materials, but in practice it has shown to be more complicated in several respects. Techniques that have satisfactorily been applied to bulk material in order to investigate excited states, and have thus determined impurity binding energies very accurately, have proved to be difficult to transfer directly to QW's. In the present work we have combined two independent spectroscopic techniques to study the transitions between the ground state and the excited states of an acceptor confined in a narrow QW. The resonant Raman scattering (RRS), as well as the so-called two-hole transition (THT) measured in PL, are both well documented from corresponding measurements on donors and acceptors in bulk material. However, much less has been reported on measurements of confined impurities using the same techniques. RRS has been reported on confined donors<sup>6</sup> and acceptors,<sup>8</sup> but to the best of our knowledge, the THT is reported here for the first time. The results provided from these spectroscopic studies showing transitions from the ground state to excited states of the same parity are then compared with theoretical predictions.<sup>10,11</sup>

### EXPERIMENT

#### Samples

The GaAs/AlGaAs QW's used in this study were all grown by MBE on semi-insulating (100) GaAs substrates with a 0.35-μm buffer layer including a smoothing superlattice, on top of the substrate. Growth temperature was

nominally around 580°C. Most samples contained a single QW (SQW), but also multiple QW's (MQW's) with up to 100 periods of doped QW's were characterized. The QW widths were in all cases close to 70 Å and the Al composition of the barriers was kept at  $x \approx 0.3$ . The samples were doped with Be in the central  $\frac{1}{4}$  of the QW in the range  $3 \times 10^{16} - 2 \times 10^{17} \text{ cm}^{-3}$ . The uniformity of the layers, determined by PL measurements at different spots on the wafer, was in most cases of the order  $\pm 2$  monolayers.

### Spectroscopy

The optical excitation for the PL experiments was from an Ar-ion laser, while the excitation for the RRS and selective PL (SPL) measurements was from a cw dye laser. The dye Styryl 8 was used in the dye laser, which could be scanned with a stepping-motor arrangement in order to do PL excitation (PLE) measurements. The samples were placed in a cryostat, in which the temperature could be varied in the range 1.4–300 K. The light, emitted perpendicular to the incident beam, was focused on the slit of a 1-m monochromator. In order to avoid reflected laser light entering the monochromator, the sample was rotated slightly off 45° relative to the incident light. The output light from the monochromator was detected with a cooled GaAs photomultiplier tube, from which the output signal was collected and computer processed.

### RESULTS

Data for two different samples will be presented in this section: Sample *A* contains a SQW, which is 70 Å wide, with Be doping at a concentration of  $1 \times 10^{17} \text{ cm}^{-3}$  in the central 25% of the QW, while sample *B* is a MQW with 100 periods of wells of intentionally the same width and doping as sample *A*. The barriers between the wells in sample *B* consisted of 200 Å  $\text{Al}_{0.3}\text{Ga}_{0.7}\text{As}$ . A PL spectrum for sample *A* with above-band-gap excitation is shown in Fig. 1. For this sample, the FE is well resolved from the BE with a separation of 4.5 meV and no further luminescence related to this QW can be detected with above-band-gap excitation. In the corresponding PL spectrum for sample *B* the linewidth has increased due to the inhomogeneity broadening in the MQW, so that the FE and BE peaks are barely resolved.

A PLE spectrum with the detection resonant with the FE emission is almost identical with a corresponding spectrum with the detection resonant with the BE peak (Fig. 2). The two narrow peaks observed in this spectrum correspond to the heavy-hole (hh) and light-hole (lh) states related to the FE. It should be noted that no additional structure originating from the BE could be observed in this sample upon detection resonant with the low-energy part of the BE peak.

A SPL spectrum with dye-laser excitation resonant with (Fig. 3) or close to (Fig. 4) the FE states observed in the PLE spectrum is quite different from the PL spectrum with above-band-gap excitation as shown in Fig. 1. First, the FE and BE peaks are not well resolved, but

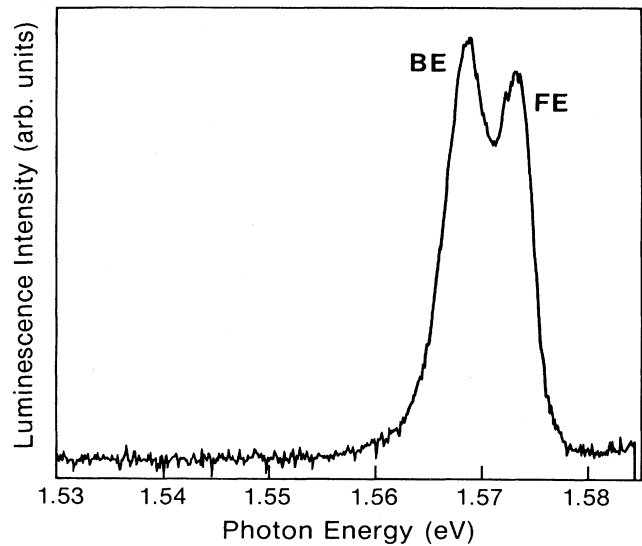


FIG. 1. PL spectrum of sample *A* at 2 K, excited with above-band-gap excitation (5145 Å). This sample has a 70-Å-wide SQW, which is Be doped in the central 25% of the well to a level of  $1 \times 10^{17} \text{ cm}^{-3}$ . The FE and BE peaks are separated by 4.5 meV.

merge into a broader joint exciton peak. It is possible, however, to observe the shift of this joint exciton peak between the two “extreme points” at  $\approx 1.574 \text{ eV}$  corresponding to the FE and  $\approx 1.569 \text{ eV}$  for the BE, as the excitation energy is shifted (as can partially be observed in Figs. 3 and 4). Furthermore, a strong peak appears at 1.550 eV for this sample (Fig. 3). Luminescence at this energy position has earlier been reported for wells with

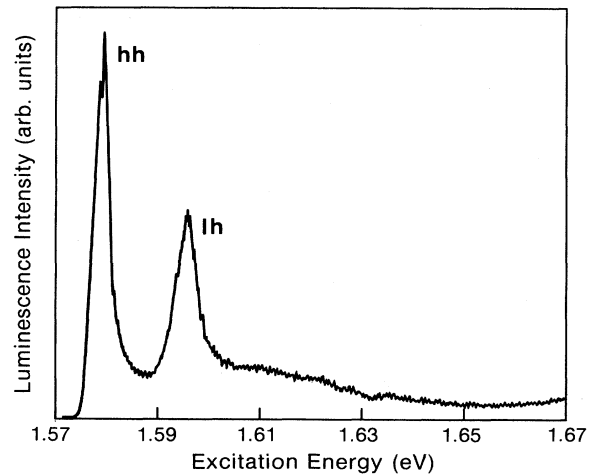


FIG. 2. PLE spectrum of sample *A* (SQW) at 2 K with detection in the BE peak. The same spot of the sample as used for the PL in Fig. 1 is intentionally focused, but since another excitation source has to be used, a small energy shift may occur. This spectrum is almost identical with the corresponding PLE spectrum, when the FE is detected. The two strong peaks in this spectrum are the two lowest FE states, the hh and lh states.

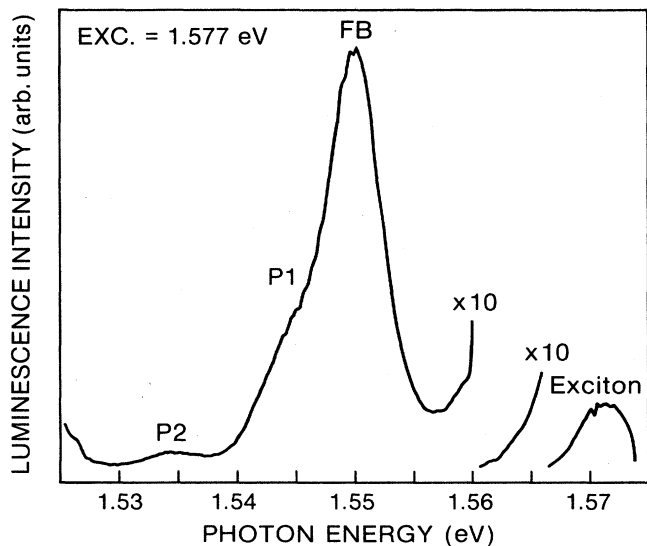


FIG. 3. SPL spectrum of sample *A* with the excitation energy resonant with the hh state of the FE. Since the focused spot of the sample might be somewhat different than what was used in Figs. 1 and 2, direct comparison of energies should proceed cautiously. As observed, the FE and BE peaks are no longer resolved at this excitation, but merge into a band peaking at  $\approx 1.572$  eV. Towards lower energies, the spectrum is dominated by a strong FB peak. As a shoulder on the low-energy side of the FB, another peak, *P1* can be observed, and at still lower energy, a weak feature, *P2* can be seen.

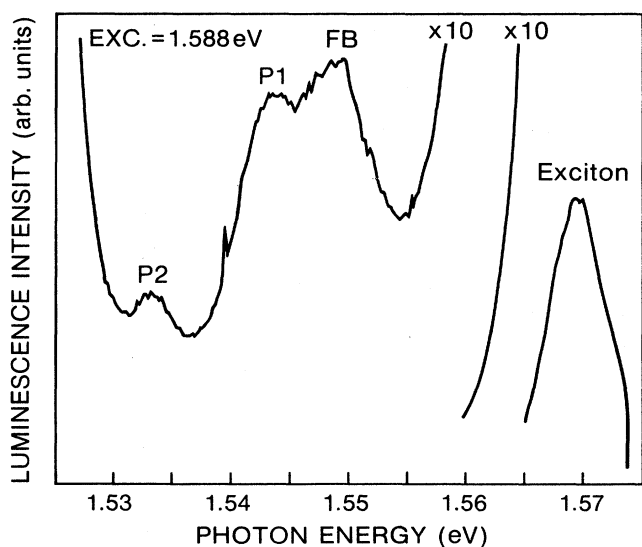


FIG. 4. The same SPL spectrum as in Fig. 3, but with non-resonant excitation. The joint exciton peak is shifted to  $\approx 1.569$  eV. Further, the intensity of the FB peak is drastically reduced and is now comparable with the *P1* peak, while the intensity ratios *P1/P2* remain unchanged.

similar doping and width<sup>2</sup> and is identified as the FB transition involving the Be acceptor. A weak peak at the same position is observed for the MQW, sample *B*, even with above-band-gap excitation (for which the FB transition is not observed in sample *A*). This is probably due to an unintentionally higher doping level in sample *B*. The position of the FB peak makes it possible to get a rough estimate of the binding energy of the Be acceptor in this QW. If the binding energy of the FE, assumed to be 11 meV,<sup>12</sup> is added to the FE transition energy, 1.574 eV, the energy separation between the ground states of the electron and the hh can be estimated to be 1.585 eV, excluding the effects of the Stokes shift observed for the FE between luminescence and excitation spectra.<sup>13</sup> The FB peak is then shifted about 35 meV from the band gap, which thus corresponds to the binding energy of the Be acceptor at the center of a 70-Å-wide QW. This is in agreement with earlier reports,<sup>2</sup> where estimates have been performed in a similar way. The strong enhancement of the FB peak, when the excitation is resonant with the hh state, can also be observed upon excitation resonant with the lh state related to the FE.<sup>2,14</sup> In addition to the strong FB peak, a fairly weak feature, *P1*, can be observed as a shoulder on the low-energy side of the FB peak and another peak, *P2*. These two peaks, *P1*, and *P2*, are interpreted as the THT's related to the BE. The energy separation from the BE is about 28.5 and 37.0 meV, respectively. These THT's will be further expounded below. As mentioned above, the FE and BE peaks have merged into a broader peak at this selective excitation, but from the position of the joint peak, one can, however, conclude that the free exciton dominates at this excitation.

When the excitation is shifted slightly off the resonance with the hh state (or the lh state) the intensity of the FB peak is drastically reduced and becomes comparable with *P1*, while the intensity ratio between *P1* and *P2* remains almost the same (Fig. 4). An important observation in this SPL spectrum (of sample *A*) is the shift of the joint exciton peak, compared with the spectrum for which the hh state was resonantly excited (Fig. 3). The position of the joint exciton peak is, in the case of excitation resonant with the hh or lh state, very close to the FE (Fig. 3), while the joint exciton peak is approaching the BE position upon the off-resonance excitation shown in Fig. 4. From many measurements of this kind there seems to be a general intensity correlation between the FE and FB peaks on one hand, and between the BE and *P1* and *P2* features on the other. The last correlation is of course an important support for the interpretation of the *P1* and *P2* peaks as originating from THT's.

The strong correlation between the FE and FB transition is even more evident in a PLE spectrum with the detection at the FB peak [Fig. 5(a)]. The hh and lh states related to the FE show up to be extremely strong and sharp, with a half-width of 1.5 meV for the hh state and 2.5 meV for the lh state. The corresponding PLE spectrum with the detection resonant with *P1* [Fig. 5(b)] shows just the same hh and lh states of the FE. These peaks are, however, considerably weaker at this detection (the intensity of the peaks versus the background is

significantly reduced). These observations are consistent with the above-stated intensity correlation between the FE and FB. From these two PLE spectra it is also apparent that the best excitation condition to get the THT peaks,  $P1$  and  $P2$ , strong in comparison with the FB peak is to use slightly nonresonant excitation. It should also be noted that no further structure which could be inferred to be of extrinsic origin could be observed in the PLE spectra.

The corresponding PLE spectrum for the MQW, sample  $B$ , shows the same hh and lh states related to the FE as observed for the SQW, sample  $A$ , but broadened due to the increased inhomogeneity in the same way as observed in PL. However, when detecting the  $P1$  peak, a weak but sharp feature appears on the low-energy side of the hh state. Further, this peak is observed to shift with

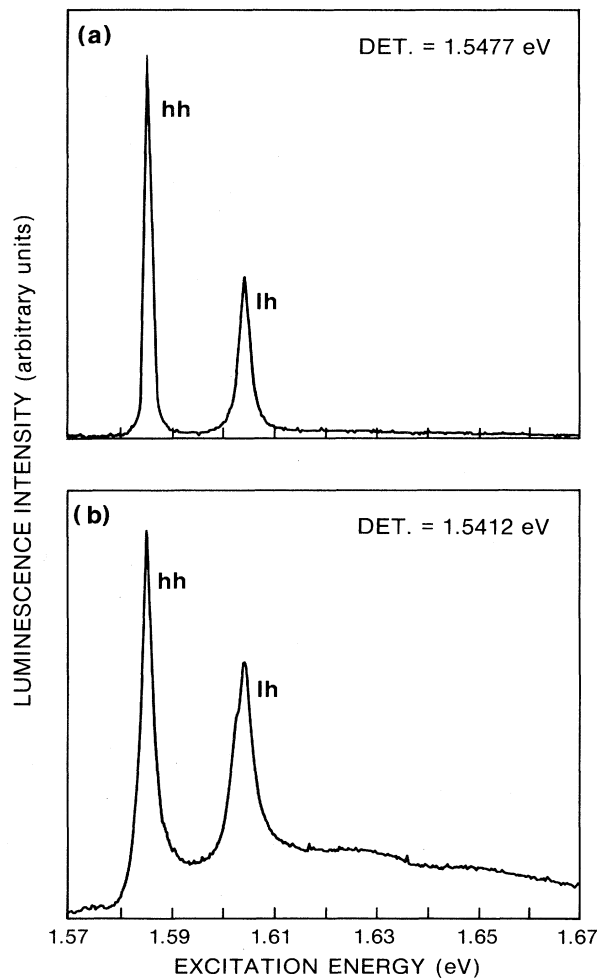


FIG. 5. PLE spectra of sample  $A$  at 2 K, when detecting (a) the FB peak and (b) the  $P1$  peak. The peaks originating from the hh and lh states of the FE are the only observed lines in both cases. These peaks are much stronger compared to the background, and are quite sharp when the FB is detected (hh- and lh-state half-widths of 1.5 and 2.5 meV, respectively).

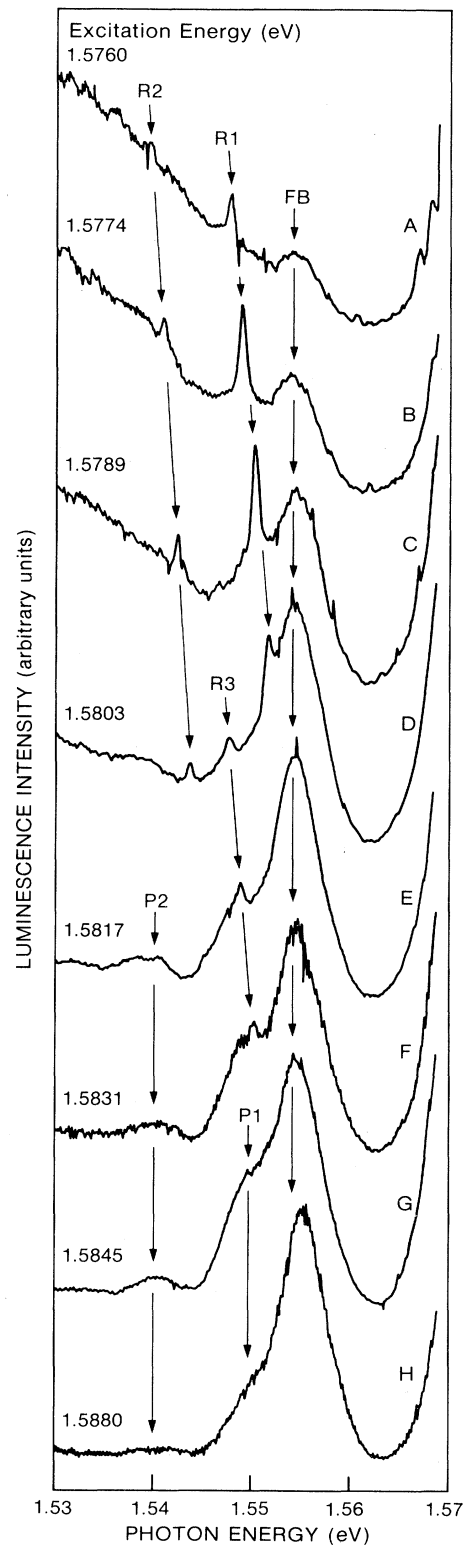


FIG. 6. A synopsis of SPL spectra for sample  $B$  at 2K, where the excitation energy is varied from 1.576 to 1.588 eV. The FB,  $P1$ , and  $P2$  peaks all stay at a fixed energy position, while the Raman-active components  $R1$ ,  $R2$ , and  $R3$  shift with the excitation energy.

the detection energy, so the energy separation between this peak and the detected energy is the same at all times. The behavior of this transition is more clear in a SPL measurement (Fig. 6). With selective excitation in the vicinity of the exciton peak, a strong and sharp peak, *R1* (with a half-width of the order 1 meV), appears close to the position of *P1*, and another sharp peak, *R2*, is observed in the vicinity of *P2*. Both these peaks seem to be Raman active and shift with the excitation energy in such a way that the energy separations between the excitation energy and the two peaks, *R1* and *R2*, are constant  $29.0 \pm 0.5$  and  $36.5 \pm 0.5$  meV, respectively. These two Raman-active peaks are strongest when the excitation is at about 1.578 eV; their intensity decreases symmetrically when the excitation is shifted to higher or lower energy, as summarized in Fig. 7. The half-width of the cross section for excitation of this Raman-active transition is  $\approx 4.5$  meV, which is of the same order as the exciton half-width in this sample. When the excitation is shifted further towards lower energy,  $\approx 1.575$  eV, all PL features disappear. If the excitation is instead shifted towards higher energy, the *R1* and *R2* peaks disappear at an excitation energy of  $\approx 1.581$  eV. The two broader features, the THT peaks, *P1* and *P2*, are, however, still observed in this excitation energy, but they decrease in intensity successively with increasing excitation energy; and are above  $\approx 1.59$  eV almost undetectable.

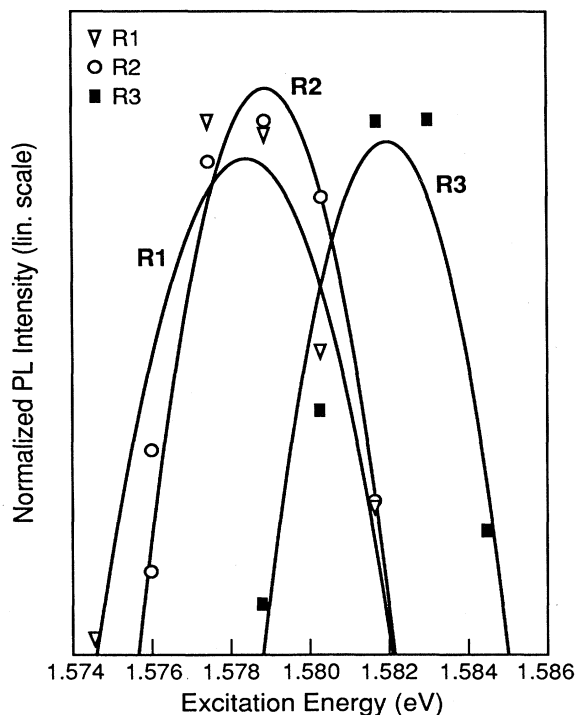


FIG. 7. The PL intensity of the Raman-active lines, *R1*, *R2*, and *R3*, as a function of excitation energy. The curves are the least-squares fit to the experimental points. The excitation cross section for the lines *R1* and *R2* peaks about 4 meV below the corresponding maximum for the *R3* peak.

Another Raman-active feature, *R3*, can also be observed in the same set of spectra (Fig. 6). That peak is shifted 32.8 meV from the excitation energy, but the cross section for excitation of this line has its maximum at  $\approx 1.582$  eV, thus at an energy 4 meV above the corresponding peak for *R1* and *R2*. The energy 1.582 eV is very close to the FE energy as observed in a PL spectrum and the energy separation, 4 meV, is the same as the separation between the FE and BE. This strongly suggests that *R1* and *R2* originate from RRS at excitation resonant with the BE, while the *R3* peak is the similar RRS component scattered via the FE. We are currently working on an investigation of the origin of the *R3* peak, which we will publish in a separate paper.<sup>15</sup> Tentatively, we interpret the *R3* line as an intrinsic THT involving the FE, in which the second hole is excited from the  $n = 1$  hh ground state to the first excited  $n = 2$  hh state.

SPL measurements performed at different temperatures show a very similar thermal behavior of the luminescence intensity for the following peaks: The BE, *P1*, *P2*, *R1*, and *R2* lines. The intensity of all these peaks starts to decrease at fairly low temperatures ( $\approx 10$  K) and the above-mentioned transitions are completely quenched at 25–30 K. The temperature dependence measurements are summarized in Fig. 8.

In order to explore the possibility that *P1* could be identified as the donor-acceptor pair (DAP) transition, in-

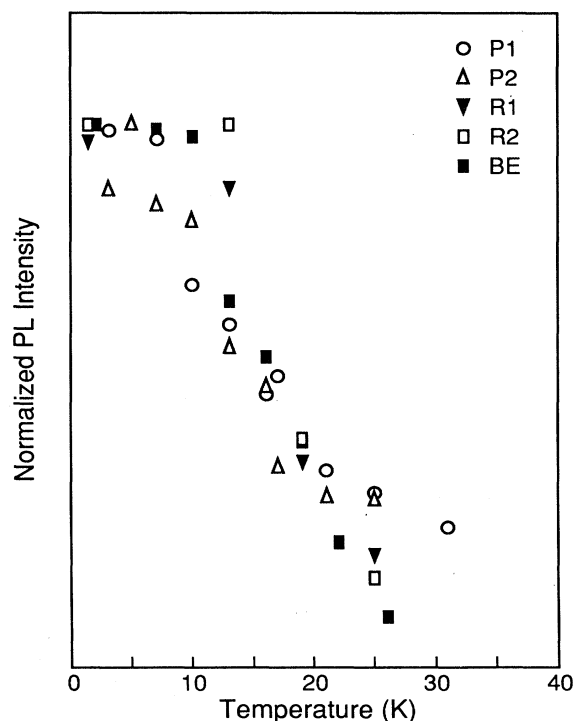


FIG. 8. The temperature dependence for the spectral lines designated BE (bound exciton), *P1* and *P2* (THT), and *R1* and *R2* (RRS).

volving the Be acceptor and a shallow donor, the excitation intensity dependence for this peak was measured. In spite of the difficulty in separating the P1 and FB peaks, it can be stated that no detectable energy shift could be observed upon changing the excitation intensity by 3 orders of magnitude. For DAP in bulk material a strong dependence of peak energy on the excitation intensity is expected. Since no corresponding studies have been performed on QW's, the most relevant comparison should be with shallow DAP's in bulk GaAs, where a shift of about 0.5 meV per order of magnitude has been reported.<sup>16</sup>

### ACCEPTOR IN A QUANTUM WELL

Calculating the energy levels of acceptors in bulk material is somewhat more complicated than in the case of donors due to the more complex valence band. In the case of donors, the electron states can be assumed to be formed by Bloch states from a single conduction band, while for acceptors one has to take into account the fact that the hole wave function is derived from states associated with several valence bands. However, at  $k=0$ , these states are degenerate in the absence of the spin-orbit interaction. Thus the upper states of the GaAs valence band consists of three  $p$ -like, triply degenerate states at  $k=0$ . When spin is included, the degeneracy of this band will be sixfold. For the calculation of energy levels of a shallow, effective-mass-like acceptor, the Hamiltonian  $H_0$  is given by<sup>11</sup>

$$H_0 = \frac{1}{2m_0}(\gamma_1 + \frac{5}{2}\gamma_2)p^2 - \frac{\gamma_2}{m_0}(p_x^2 J_x^2 + p_y^2 J_y^2 + p_z^2 J_z^2) - \frac{2\gamma_3}{m_0}(\{p_x p_y\}\{J_x J_y\} + \{p_y p_z\}\{J_y J_z\} + \{p_z p_x\}\{J_z J_x\}) - \frac{e^2}{\epsilon_0 r} \quad (1)$$

where  $\gamma_1$ ,  $\gamma_2$ , and  $\gamma_3$  are the Luttinger parameters of the valence band,  $\{ab\} = (ab + ba)/2$ ,  $m_0$  is the free electron mass,  $p$  is the linear momentum operator, and  $J$  is the angular momentum operator for the spin- $\frac{3}{2}$  hole.

When a shallow acceptor with the symmetry of the tetrahedral group  $T_d$  is introduced in bulk material, the  $p$ -like band will transform like  $\Gamma_5$ . To deduce the valence-band symmetry, this  $\Gamma_5$  state of the  $p$ -like band should be coupled with the  $\Gamma_6$  state representing the  $j = \frac{1}{2}$  spin state. According to group theory this spin-orbit coupling will give rise to  $\Gamma_5 \times \Gamma_6 = \Gamma_7 + \Gamma_8$ . Thus the sixfold degenerate band will split into two bands, one twofold degenerate ( $\Gamma_7$  band) and one fourfold degenerate ( $\Gamma_8$  band). Away from  $k=0$ , the upper  $\Gamma_8$  band will split further into two Kramers doublets, a twofold degenerate light-hole band and a twofold degenerate heavy-hole band.

In the case of a QW potential, the symmetry will be reduced from  $T_d$  to  $D_{2d}$ . If the same calculations are performed for this lower symmetry,  $D_{2d}$ , as for the  $T_d$  symmetry,<sup>11</sup> it can be shown that the fourfold degenerate  $\Gamma_8$  band will split into two twofold degenerate bands even at  $k=0$  in the QW, the light-hole band with symmetry  $\Gamma_7$

and heavy-hole band with symmetry  $\Gamma_6$ . To calculate the energy levels of such an acceptor, an extended Hamiltonian  $H$ , compared with the one used for bulk material [Eq. (1)] must be used:

$$H = H_0 + V_c(r) + H_1(z) . \quad (2)$$

Thus the  $H_1(z)$  and  $V_c(r)$  terms have been added to the Hamiltonian used for bulk material [Eq. (1)]. The  $H_1(z)$  term refers to the potential energy for the barriers:

$$H_1(z) = \begin{cases} 0 & \text{for } z \text{ in the well} \\ V_0 & \text{for } z \text{ in the barrier} \end{cases}$$

where  $V_0$  corresponds to the discontinuity of the valence band.  $V_c$  is the so-called central-cell potential due to different chemical shift for different acceptors. Masselink *et al.*<sup>11</sup> have calculated the subband states and the acceptor states using the variational method with the above Hamiltonian [Eq. (2)]. The calculations were performed separately for the  $\Gamma_6$  and  $\Gamma_7$  hole states. The resulting energy levels for an acceptor in the center of a QW with barriers having Al content of  $x=0.30$  (as is the case for the samples studied here) are given in Fig. 9. As can be observed in this figure, the binding energy of the  $\Gamma_7$  ground state will increase compared with the binding energy of the  $\Gamma_6$  state for a QW. Further, it can be seen that the effect of the confinement increases the binding energy with the narrowing of the QW. However, the binding energy for the  $\Gamma_6$  and  $\Gamma_7$  will go through a maximum at some nonzero well width. This occurs at  $\approx 10 \text{ \AA}$  for the  $\Gamma_6$  state and at  $\approx 25 \text{ \AA}$  for the  $\Gamma_7$  state.<sup>10,11</sup> When the well width is zero (corresponding to

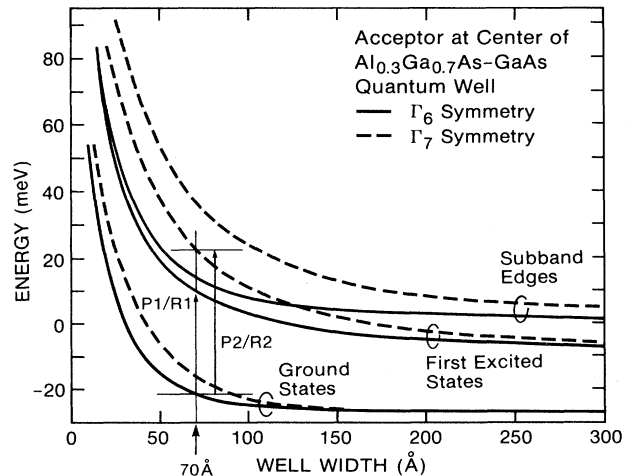


FIG. 9. The QW width dependence of some of the states of an acceptor at the center of a QW, based on the calculations by Masselink *et al.* (Ref. 10). The energy zero on the vertical axis corresponds to the bulk valence-band edge. The labeled transitions refer to the corresponding transitions as observed in our THT and RRS experiments.

the case of bulk AlGaAs), the binding energy is, of course, the same as in AlGaAs.

### DISCUSSION

In this study we have observed two well-defined lines in SPL corresponding to transitions from the ground state to two different excited states of a Be acceptor confined in a narrow QW. These transitions are observed in SPL in two different ways: THT (lines *P1* and *P2*), when the excitation energy is in the range of the FE, and RRS (lines *R1* and *R2*) for excitation resonant with the BE. The observation of RRS and THT for the same impurity has earlier been seen in bulk material.<sup>17</sup> The observed lines appear in the same spectral range, but differ in the SPL spectra in some important respects: The *R1* and *R2* lines shift with the excitation energy, and they are, in addition, much sharper than the *P1* and *P2* peaks. Further, as mentioned above, the *P1* and *P2* peaks are strongest when the excitation energy is resonant with or close to the FE, while the *R1* and *R2* lines are just observed upon excitation resonant with the BE.

The *P1* and *P2* peaks are interpreted as the THT states originating from the recombination of the BE. There is a (small) probability that part of the recombination energy is transferred to the acceptor, which is left in an excited state. The recombination energy is then reduced by the energy needed to excite the acceptor. The THT peak will thus be at a constant energy separation from the BE. The width of the THT peak should then be of the same order as the BE, in agreement with what is experimentally observed.

A PLE spectrum with detection at either of the THT peaks, *P1* or *P2*, does not show a strong BE peak, in contrast to what is observed in bulk material. However, the same observation can be made, when detecting the low-energy part of the BE itself; similarly in this case, the PLE spectrum is dominated by the FE-related peaks. This is consistent with the PL, where the FE is usually the dominating peak in a QW, in contrast to the bulk, where the BE is normally stronger. The strong FE in a QW is usually explained by its shorter lifetime compared with the bulk, due to the increasing overlap between the electron and hole wave functions as the confinement increases. This may also explain the domination of the FE-related peaks in the PLE spectra.

The *R1* and *R2* peaks are interpreted as due to RRS, which is, as the name implies, a scattering process, where an incoming photon is inelastically scattered via the acceptor, which is left in an excited state. This leads to a reduction in the energy of the outgoing photon by an amount corresponding to the energy needed to excite the acceptor. Thus there will be a constant energy separation between the excitation energy and the RRS peak. The width of the RRS line is determined by the distribution of the acceptor binding energies. This distribution is due to the different positions of the acceptors in the QW and is in our case, with doping in the central  $\frac{1}{4}$  of the well, of the order 2 meV.<sup>9,10</sup> The width of the excitation cross section for the RRS process, on the other hand, should be of the same order as the scattering source, i.e., the BE

peak. All these predictions are in good agreement with what is observed experimentally (Figs. 1, 6, and 7).

An alternative explanation for the *R1* and *R2* transitions as being due to another THT cannot be ruled out at the present stage.<sup>18</sup> Such a THT process should be more similar to what is seen in bulk material, with the intensity enhancement observed upon excitation resonant with the BE. This is in contrast to the *P1* and *P2* peaks, which are most efficiently excited via the FE states. The different properties (regarding the shift with the excitation energy and the small linewidth) of the *R1* and *R2* lines should be found in the selective excitation of different parts of the distribution of BE states. Due to the interface roughness, there will always be a distribution of "effective" QW widths, which gives rise to the broadening of the exciton peak compared with bulk material. With the resonant dye-laser excitation at a certain energy in this exciton peak, just a minor part of this energy distribution can be selected, corresponding to a more narrow range of QW widths. When the excitation energy is shifted within the exciton peak, a slightly different QW width is selected, which, in turn, gives rise to a new THT peak shifted in the same way as the excitation (the corresponding shift of the acceptor binding energy is negligible). These facts explain the small linewidths of the *R1* and *R2* lines as well as the shift of these lines with the excitation energy. The reason for the observation of the *R1* and *R2* lines in just the MQW is not known for the moment. New SQW's will be grown in order to exclude any "unknown growth parameter" as the origin of these discrepancies.

The temperature dependences for the *P1*, *P2*, *R1*, and *R2* lines are very similar and also almost identical with the thermal behavior of the BE (Fig. 8). The intensity reduction of these lines starts at about 10 K and they are completely quenched at  $\approx 30$  K. It can thus be concluded that the temperature dependence of the *P1*, *P2*, *R1*, and *R2* transitions seems to reflect the thermal behavior of the BE.

The selection rules, which apply for RRS as well as THT in the case of acceptors in bulk material, strongly favor transitions between states of the same parity, i.e., mainly from the  $1s_{3/2}$  ground state to *s*-like excited states.<sup>19</sup> Accordingly, for the case of impurities confined in a QW, the strongest line observed in RRS is ascribed to the  $1s_{3/2}$ - $2s_{3/2}$  transition for donors<sup>6</sup> as well as for acceptors.<sup>8</sup> Furthermore, when the acceptors are introduced into a QW instead of into bulk material, the symmetry is reduced from  $T_d$  to  $D_{2d}$ . In that case, all possible transitions between different symmetries (i.e.,  $\Gamma_6$ - $\Gamma_6$ ,  $\Gamma_7$  and  $\Gamma_7$ - $\Gamma_6$ ,  $\Gamma_7$ ) could be expected if higher-order terms (at least quadratic) are taken into account. This is a reasonable assumption based on the fact that both the RRS and THT processes are of resonant character.<sup>8</sup> In fact, similar transitions between Kramers doublets of different symmetry ( $\Gamma_6$  and  $\Gamma_7$ ) have been observed in RRS also for bulk GaP under stress.<sup>20</sup>

Based on the facts stated above, the interpretation of the strongest of the observed lines, *P1* and *R1* in THT and RRS, respectively, is the  $1s_{3/2}[\Gamma_6]$ - $2s_{3/2}[\Gamma_6]$  transition of the confined Be acceptor. There is good agree-

ment between the transition energies observed in THT ( $28.5 \pm 1$  meV) and in RRS ( $29.0 \pm 0.5$  meV). The experimental observations are also consistent with theoretical predictions,<sup>10</sup> where the calculated energy for the same transition for an effective-mass-like acceptor confined in a 70-Å well is  $\approx 30$  meV. The central-cell correction corresponding to the difference in binding energy of the  $1s$  ground state between the Be acceptor and an effective-mass-like acceptor is about 2 meV for the bulk. Assuming the same central-cell correction can be used for the confined acceptor gives a calculated transition energy for the confined acceptor of 32 meV. Using the same central-cell factor gives a calculated ionization energy of 36 meV for the  $\Gamma_6$  symmetry compared with the estimated 35 meV from the position of the FB peak.

The interpretation of the second peak,  $P2$  and  $R2$  in the two-hole and Raman spectra, respectively, is not that obvious. One possible explanation for the line is the transition to the next  $s$ -like excited state,  $1s_{3/2}[\Gamma_6]-3s_{3/2}[\Gamma_6]$ . The observed energy separation between  $P1$  ( $R1$ ) and  $P2$  ( $R2$ ), 8 meV, seems to be too large, however, based on a comparison with bulk, where the corresponding transition is less than 4 meV.<sup>21</sup> Furthermore, the effect of increased confinement due to the well should decrease this number, not increase it.<sup>10</sup> This explanation must therefore be ruled out. Likewise the assignment of the  $P2$  and  $R2$  lines as the transition from the  $1s_{3/2}[\Gamma_6]$  to the subband edge can also be ruled out for two reasons: firstly, the same kind of energy considerations as mentioned above should be applicable, and secondly, a line originating from a well-defined state to a subband is expected to broaden compared with a transition to a single level. Another possibility should be to interpret  $P2$  and  $R2$  as phonons, since the observed transition energy is very close to the LO-phonon energy in GaAs. Also this interpretation seems to be unlikely for different reasons: Firstly, the behavior of  $P2$  and  $R2$  is very similar to what is observed for  $P1$  and  $R1$ , which indicates a similar origin. Secondly, it should assume phonon coupling to just the BE and not the FE (which still is possible, however). The third argument is the comparison with QW's of varying widths, where the corresponding transition energy has been observed in somewhat wider QW's at a slightly lower transition energy.<sup>16</sup> However, it should also be pointed out that SPL measurements have been performed on other QW's without observing peaks originating from this transition, but only from the stronger  $1s_{3/2}[\Gamma_6]-2s_{3/2}[\Gamma_6]$  transition. This fact is most probably due to the relatively low oscillator strength for this transition. We therefore conclude that the most plausible interpretation of the  $P2$  and  $R2$  lines as an electronic transition between different symmetries,  $1s_{3/2}[\Gamma_6]-2s_{3/2}[\Gamma_7]$ . Furthermore, when one considers the appropriate selection rules<sup>8</sup> the assignment of the  $P2$  and  $R2$  lines as the transition,  $1s_{3/2}[\Gamma_6]-2s_{3/2}[\Gamma_7]$ , seems to be the most reasonable one. According to the theoretical work by Masselink *et al.*<sup>10</sup> the energy for this transition is about 42 meV. With the above-assumed central-cell correction, the calculated transition energy is  $\approx 44$  meV, which should be compared with the experimental estimate,  $36.5 \pm 0.5$  meV, in RRS and  $37.0 \pm 1$  meV in THT, respectively.

Because the energies of impurity states of different symmetry are strongly affected by band-structure effects, for which theoretical calculations have limited accuracy (10–15 % error in these calculations is not unexpected), the observed agreement between the experiments reported here and the predictions quoted is felt to be quite good. In fact, if the proposed assignment of these states is correct (cf. discussion above), then the extremely close agreement between the two different phenomena for which this transition is observed (RRS and THT) suggests that the experimentally determined energies are the correct ones, providing the theorists with extremely accurate data points for further calculation.

## SUMMARY

The Be acceptor, confined to the central part of a narrow (70 Å) GaAs/AlGaAs QW, has been studied using two different spectroscopic methods: two-hole transitions (THT) of the BE and resonant Raman scattering (RRS). In both cases selective dye-laser excitation was used. Two well-defined peaks at about the same energy position in RRS as well as THT have been observed, when selective excitation is employed in the exciton range. The observed lines are assigned to transitions from the ground state,  $1s_{3/2}[\Gamma_6]$ , to two different excited states,  $2s_{3/2}[\Gamma_6]$  and  $2s_{3/2}[\Gamma_7]$ . The fact that the two transitions can be observed in two different ways at very similar energies is convincing for the interpretation of the observed transitions. Furthermore, the temperature dependences for the RRS and THT peaks are very similar, and almost identical with the thermal behavior of the BE, which also supports the relationship between the observed transitions and the BE. The cross section for excitation of the RRS lines is observed to reach a maximum at about 4 meV lower energy than another Raman-active line, which results from photon scattering via the FE; this result provides further support for the interpretation that the stronger lines discussed above occur via Raman scattering involving the BE. The observed transition energies for the two lines,  $29.0 \pm 0.5$  and  $36.5 \pm 0.5$  meV in RRS and  $28.5 \pm 1$  and  $37.0 \pm 1$  meV in THT, are very well defined; comparison with theoretical calculations is therefore of high interest. The only reported calculation of acceptor states in GaAs/AlGaAs QW's, by Masselink *et al.*,<sup>10</sup> predicts transition energies of 32 and 44 meV for the two observed transitions of an acceptor confined in a 70-Å-wide well after correction for the central-cell effect.

## ACKNOWLEDGMENTS

The authors are grateful to Professor M. L. W. Thewalt for useful discussions. One of the authors (P.O.H.) is supported by the Swedish Natural Science Research Council. This work was partially supported by the Defense Advanced Research Projects Agency (DARPA Contract No. N00014-87-K-0365) and by the Semiconductor Research Corporation.



- \*Permanent address: Department of Physics and Measurement Technology, Linköping University, 58183 Linköping, Sweden.
- <sup>1</sup>R. C. Miller, A. C. Gossard, W. T. Tsang, and O. Munteanu, *Phys. Rev. B* **25**, 3871 (1982).
- <sup>2</sup>R. C. Miller, *J. Appl. Phys.* **56**, 1136 (1984).
- <sup>3</sup>Ronald L. Greene and Pat Lane, *Phys. Rev. B* **34**, 8639 (1986).
- <sup>4</sup>R. C. Miller, A. C. Gossard, W. T. Tsang, and O. Munteanu, *Solid State Commun.* **43**, 519 (1982).
- <sup>5</sup>N. Balkan, B. K. Ridley, J. Frost, D. A. Andrews, I. Goodridge, and J. Roberts, *Superlatt. Microstruct.* **2**, 357 (1986).
- <sup>6</sup>B. V. Shanabrook, J. Comas, T. A. Perry, and R. Merlin, *Phys. Rev. B* **29**, 7096 (1984).
- <sup>7</sup>D. C. Reynolds, K. K. Bajaj, C. W. Litton, P. W. Yu, W. T. Masselink, R. Fisher, and H. Morkoç, *Phys. Rev. B* **29**, 7038 (1984).
- <sup>8</sup>D. Gammon and R. Merlin, *Phys. Rev. B* **33**, 2919 (1986).
- <sup>9</sup>G. Bastard, *Phys. Rev. B* **24**, 4714 (1982).
- <sup>10</sup>W. T. Masselink, Yia-Chung Chang, and H. Morkoç, *Phys. Rev. B* **32**, 5190 (1985).
- <sup>11</sup>W. T. Masselink, Y.-C. Chang, H. Morkoç, D. C. Reynolds, C. W. Litton, K. K. Bajaj, and P. W. Yu, *Solid-State Electron.* **29**, 205 (1986).
- <sup>12</sup>P. Dawson, K. J. Moore, G. Duggan, H. I. Ralph, and C. T. B. Foxon, *Phys. Rev. B* **34**, 6007 (1986).
- <sup>13</sup>G. Bastard, C. Delande, M. H. Meynadier, P. M. Frijlink, and M. Voos, *Phys. Rev. B* **29**, 7042 (1984).
- <sup>14</sup>P. O. Holtz, M. Sundaram, R. Simes, J. L. Merz, and A. C. Gossard (unpublished).
- <sup>15</sup>P. O. Holtz, M. Sundaram, J. L. Merz, and A. C. Gossard, (unpublished).
- <sup>16</sup>J. van de Ven, H. G. Schoot, and L. J. Giling, *J. Appl. Phys.* **60**, 1648 (1986).
- <sup>17</sup>P. O. Holtz, B. Monemar, H. P. Gislason, Ch. Uihlein, and P. L. Liu, *Phys. Rev. B* **32**, 3730 (1985).
- <sup>18</sup>M. L. W. Thewalt (private communication).
- <sup>19</sup>P. Y. Yu, *Phys. Rev. B* **20**, 5286 (1979).
- <sup>20</sup>C. H. Henry, J. J. Hopfield, and L. C. Luther, *Phys. Rev. Lett.* **17**, 1178 (1986).
- <sup>21</sup>J. C. Garcia, A. C. Beye, J. P. Contour, G. Neu, J. Massies, and A. Barski, *Appl. Phys. Lett.* **52**, 1596 (1988).